Characterization of soft-sediment deformation: Detection of crypto-slumps using magnetic methods

Kurt Schwehr
Lisa Tauxe
Scripps Institution of Oceanography, University of California San Diego, La Jolla, California 92093-0208, USA

ABSTRACT

Many workers have explored anisotropy of magnetic susceptibility (AMS) of sediments as an indicator of deformation. Several studies have used deflection of the eigenvector associated with the minimum in susceptibility $\mathbf{V}_3$ as a criterion for deformation. We examine the AMS record of a well-exposed slump and find that although demonstrable deformation can occur without deflecting the $\mathbf{V}_3$ directions, an oblate AMS fabric is transformed into a triaxial fabric during initial deformation. Transformation of the fabric from oblate to triaxial appears to be highly correlated with an increase in NRM scatter, whereas deflection of the $\mathbf{V}_3$ axes is not. We suggest that subtle soft-sediment deformation can be detected by using AMS fabric.

Keywords: Ardath Shale, soft-sediment deformation, anisotropy of magnetic susceptibility, paleomagnetism.

INTRODUCTION

The magnetic fabric of geological materials, in particular of sediments, has been a focus of interest for decades (e.g. Ising, 1942; Granar, 1958; Rees, 1965). Given that it is extremely sensitive to strain, magnetic fabric has recently been used to detect subtle deformation of sediments and to distinguish geomagnetic features from deformational artifacts (e.g., Rosenbaum et al., 2000). Cronin et al. (2001) suggested that the anisotropy of magnetic susceptibility (AMS) could be used to detect slumps not otherwise obvious from the geologic field evidence (so-called "crypto-slumps").

A range of laboratory experiments has been done on the depositional controls of magnetic fabric and its relationship to NRM (summarized in Tauxe, 1998.) In quiet-water conditions, there is a tendency for elongate particles to lie subparallel to the bedding plane. As the magnetic susceptibility is usually at a maximum parallel to the long axis of particles, $\mathbf{V}_1$ will tend to lie within the bedding plane. [Because many articles on AMS confuse eigenvalues and eigenvectors referring to both as, for example k_{min}, we use the terminology of Tauxe, 1998 whereby the eigenvectors are denoted by $\mathbf{V}$ and the eigenvalues as τ with τ_1 being the largest and τ_3 the smallest.] There is no preferred direction within the bedding plane, however, so $\mathbf{V}_2$ and $\mathbf{V}_1$ will be indistinguishable as will the associated eigenvalues τ_2 and τ_1. Hence the magnetic fabric will be oblate with a vertical $\mathbf{V}_3$ direction.

In moderate water currents, especially on inclined bedding planes, particles may be slightly imbricated, resulting in slightly off-vertical $\mathbf{V}_3$ directions. Here too we expect the fabric to be characterized by an oblate AMS ellipsoid, but the $\mathbf{V}_3$ direction will be antiparallel to the direction of paleocurrent. Finally, when deposition occurs under high current flow, with particles entrained, the $\mathbf{V}_1$ distribution is streaked, $\mathbf{V}_1$ is perpendicular to the flow direction (Jeffrey, 1922), and the fabric is characterized by prolate or triaxial ellipsoids.

What happens to the magnetic fabric during postdepositional deformation is more complex. Initial theoretical work has been done by Owens (1974), Hrouda and Hruskova (1990), and Housen et al. (1993) on the relationship between magnetic fabrics and actual grain fabrics with respect to strain. Most studies concerning strain in relation to AMS fabric have dealt with tectonic scales (e.g., Kanamatsu et al., 2001; Pares et al., 1999) and at least weakly metamorphosed rocks. However, as suggested by Rosenbaum et al. (2000) and Cronin et al. (2001), it appears that even minor amounts of soft-sediment deformation can have a profound effect on the paleomagnetic record. Such deformation, however, can be extremely difficult to detect on the basis of visual observations alone, hence the term "crypto-slump." In this paper, we pursue the idea that soft-sediment deformation can be detected through the use of AMS by investigating both crypto-slumped sediments from a marine environment along with the sediments from within and above the slump to try to confirm observations of Cronin et al. (2001). Our crypto-slump can be traced to a slumping event along the outcrop. Without the excellent exposure along the outcrop, however, its slumped nature would not be easily detected. Our goal is to develop a robust test for deformation based on the AMS characteristics of the slumped vs. undeformed sediments.

GEOLOGIC SETTING

The Ardath Shale Formation of the La Jolla Group is part of a sequence of Eocene (49–46 Ma) rocks. The La Jolla Group was deposited within an ancient submarine channel and fan system that opened westward to the Pacific Ocean; it has since been uplifted to its present position (Kennedy, 1975; Chanpong, 1975). The Ardath Shale crops out along the base of an ~100-m-high sea cliff (Fig. 1) north of the pier at the Scripps Institution of Oceanography (La Jolla, California). Contained in the cliff are a number of cut-and-fill channel sequences that were likely sediment-transport conduits much like the Scripps Canyon head today. On the basis of data presented by May and Warme (1991), the paleocurrent direction is inferred to have been ~230°. Lohmar et al. (1979) used foraminifera to estimate the paleodepth to have been 200–600 m. This places the sedimentary environment of the Ardath Shale in the outer shelf or upper slope.

The Ardath Shale at the Scripps locality is mostly covered by modern beach sand, but extends 5 m above the beach in places. The lowest part of the exposed unit has well-defined horizontal laminations with no observed deformation. Above this, there is a 1-m-thick zone of soft-sediment deformation inferred to have been caused by slumping. There are overturned and recumbent folds up to 1 m across (Fig. 1A). The overlying part of the Ardath Shale extends for another 2 m and is well laminated and apparently undisturbed. The top of the Ardath here is an erosional unconformity with an overlying conglomerate (Fig. 1B).

SAMPLING AND ANALYSIS

We sampled three sites within and surrounding a major slump in the Ardath Shale. The geologic context of the three sites is shown in Figure 1. Site A (Fig. 1B) is located 1 m above the slump in well-laminated and visually undeformed shale. Site B (Fig. 1C) is located 50 cm below the base of the slumped interval, and site C is located in the bottom 10 cm of the slump. The sampling site for site C is a less deformed region of the slump with bedding visibly deformed, but still within 10° of the bedding above and below the slump. Cores were drilled with a gasoline-powered drill and cut into nominal 1-inch (2.5 cm) specimens.

AMS Measurements

AMS measurements were done at the Scripps Paleomagnetic Laboratory on a Kappabridge KLY-2 by using the 15-measurement scheme of Jelinek (1978). We calculated the best-fit tensor for each specimen by using Hext statistics (Hext, 1963; see also Tauxe, 1998). The directions of the eigenvectors for all specimens are shown in Figures 2A–2C. To assess the statistical distribution of these data, we used a variation of the bootstrap described by Constable and Tauxe (1990) and Tauxe (1998). The bootstrap eigenvectors for the data sets are shown in Figures 2D–2F, while the bootstrap eigenvalues are shown as histograms in Figures 2G–2I. The 95% confidence bounds for the minimum τ_3, intermediate τ_2, and maximum τ_1 eigenvalues are plotted above the each histogram.

In general, the eigenvectors associated with the minimum in magnetic susceptibility $\mathbf{V}_3$ are subvertical in all three sites. The intermediate and maximum susceptibility eigenvectors ($\mathbf{V}_2$ and $\mathbf{V}_1$, respectively) girdle the horizontal. The subtle differences in ellipsoid shape hold the key to our interpretation as to origin of the fabric.

The average eigenvector $\mathbf{V}_3$ for site A (Fig. 2A) is near vertical, but the distribution of the mean eigenvectors (Fig. 2D) shows that it is deflected an average of 12.7° toward 242.7°, in good agreement with the local paleocurrent indicators mentioned previously. The AMS (magnitude) ellipsoid is oblate as indicated by the overlap of the 95% confidence bounds of τ_1 and τ_2 in Figure 2G.

The specimen (Fig. 2B) and the bootstrap eigenvectors (Fig. 2E) for site B both show that $\mathbf{V}_2$ and $\mathbf{V}_1$ are in two distinct groups. The histogram confidence intervals of eigenvalues (Fig. 2H) show that the intermediate and maximum axes are statistically distinct; therefore the ellipsoid is classified as a weak triaxial fabric. We conclude that this sediment has been deformed by the slumping of overlying sediments that occurred while they were still soft. Cronin et al. (2001) termed this kind of deformation “crypto-slumping.”

The $\mathbf{V}_3$ directions from site C (Fig. 2C) are well grouped about the vertical. The $\mathbf{V}_1$ and $\mathbf{V}_2$ directions are also tightly grouped in the horizontal direction; $\mathbf{V}_1$ is oriented roughly perpendicular to the direction of inferred compression (east-west from the vergence of the slumps). The eigenvalues are distinctly triaxial (Fig. 2I).

Remanence Measurements

Measurements of the natural remanent magnetization (NRM) of the specimens were made by using a three-axis CTF cryogenic magnetometer, located in a magnetically shielded room. Alternating field (AF) demagnetizations were accomplished with an SI-4. NRM directions and representative vector-endpoint diagrams for demagnetizations are shown (Figs. 2J–2L). These samples were magnetically soft; measurements beyond 40 mT were highly scattered and are not shown. A typical Mr/Ms ratio for the Ardath Shale is 0.074.

The average NRM directions are summarized in Table 1. The average direction from the undeformed site (site A) is close to the expected direction for the Eocene at this locality (351.6° and 54.3°; Diehl et al., 1983). The site mean for the crypto-slump (site B) is significantly shallower than the undeformed site. That from the slump is on average steeper, but is much more scattered with a κ of 21.8 as opposed to 45.3 for the undeformed site. Without further information, it would be tempting to interpret the data from the crypto-slump as genuine field behavior.

DISCUSSION AND CONCLUSIONS

AMS fabric is sensitive to strain even in small amounts on both regional and local scales. Such strain does not have to be visible for effects to be detectable in the AMS and NRM measurements. Several authors have devised tests for sediment deformation based on AMS fabric. Shor et al. (1984) used a strict test that discards all samples with f >15°, where f is the angular deviation of $\mathbf{V}_3$ from the pole to bedding defined in Crimes and Oldershaw (1967). Rosenbaum et al. (2000) developed a similar test that also relies on the $\mathbf{V}_3$ vector. They expect "good" samples to have a standard deviation of $\mathbf{V}_3$ inclination ($\sigma_{\mathbf{V}_3}$) of <6.5° and an inclination average of $\mathbf{V}_3$ ($I_{\mathbf{V}_3}$) of <6° from the vertical. Rosenbaum et al. (2000) found that for undisturbed sections, $\sigma_{\mathbf{V}_3}$ was <6.5° and the $I_{\mathbf{V}_3}$ was 84°. For our undisturbed site (site A), we calculated $\sigma_{\mathbf{V}_3}$ to be 18.3° and $I_{\mathbf{V}_3}$ to be 72.0°. For their deformed cores, Rosenbaum et al. (2000) calculated $\sigma_{\mathbf{V}_3}$ to be 26° and $I_{\mathbf{V}_3}$ to be 66.5°, whereas we found $\sigma_{\mathbf{V}_3}$ to be 5.0° and $I_{\mathbf{V}_3}$ to be 80.9° (site C). In short, we see a relationship that is opposite to that seen by Rosenbaum et al. (2000) whereby the disturbed intervals are actually more tightly grouped and more vertical than the undisturbed interval.

Although the method outlined in Rosenbaum et al. (2000) may be able to distinguish fluidized zones, it is perhaps not the best approach for several reasons. First, the mean inclination from a set having a near-vertical direction will always be biased too low (see, e.g., Briden and Ward, 1966; Kono, 1980; McFadden and Reid, 1982). Second, eigenvectors are not independent, so the average minimum eigenvector should be estimated by using Hext (1963) statistics, not Fisher (1953) statistics. Furthermore, as discussed previously, there are many reasons why $\mathbf{V}_3$ could be deflected from the vertical other than postdepositional deformation. Finally, sediments can be severely deformed without deflecting $\mathbf{V}_3$ (see Figs. 2B–2C). The tests of Rosenbaum et al. (2000) and Shor et al. (1984) would not detect the deformation in sites B and C where $\mathbf{V}_3$ is near vertical. We propose that the eigenvalue test illustrated in Fig 2g-i is much more sensitive to deformation than $\mathbf{V}_3$ deflection.

AMS fabric provides a way to distinguish between synsedimentary structures and subsequent deformation in situations where field observations are ambiguous. Many continental-slope regions show seismic signatures that have been interpreted as either retrogressive slope failure (Gardner et al., 1999) or as depositional features associated with hyperpycnal flows (N. Driscoll, 2000, personal commun.). The presence of a deformed sedimentary fabric would be strong evidence that a structure has undergone slumping.

REFERENCES

Briden, J.C., and Ward, M.A., 1966, Analysis of magnetic inclination in borecores: Pure and Applied Geophysics, v. 63, p. 133–152.

Chanpong, R.R., 1975, Depositional environment of the Ardath Shale [M.S. thesis]: San Diego, California, San Diego State University, 176 p.

Constable, C., and Tauxe, L., 1990, The bootstrap for magnetic susceptibility tensors: Journal of Geophysical Research, v. 95, p. 8383–8395.

Crimes, T.P., and Oldershaw, M.A., 1967, Palaeocurrent determinations by magnetic fabric measurements on the Cambrian rocks of Saint Tudwal's Peninsula, North Wales: Geological Journal, v. 5, p. 217–232.

Cronin, M., Tauxe, L., Constable, C., Selkin, P., and Pick, T., 2001, Noise in the quiet zone: Earth Planetary Science Letters, v. 190, p. 13–30.

Diehl, J.F., Beck, M.E., J., Beske-Diehl, S., Jacobson, D., and Hearn, B.C., J., 1983, Paleomagnetism of the Late Cretaceous-early Tertiary North-Central Montana alkalic province: Journal of Geophysical Research, v. 88, p. 10,593–10,609.

Fisher, R.A., 1953, Dispersion on a sphere: Proceedings of the Royal Society of London, Serial A, v 217, p. 295-305.

Gardner, J., Prior, D., and Field, M., 1999, Humboldt Slide—a large shear-dominated retrogressive slope failure: Marine Geology, v. 154, p. 323–338.

Granar, L., 1958, Magnetic measurements on Swedish varved sediments: Arkiv for Geofysik, v. 3, p. 1–40.

Hext, G.R., 1963, The estimation of second-order tensors, with related tests and designs: Biometrika, v. 50, p. 353–357.

Housen, B.A., C. Richter, and van der Pluijm, B.A., 1993, Composite magnetic anisotropy fabrics: Experiments, numerical models, and implications for the quantification of rock fabrics: Tectonophysics, v. 220, p. 1–12.

Hrouda, F., and Hruskova, L., 1990, On the detection of weak strain parallel to the bedding by magnetic anisotropy: A mathematical model study: Studia Geophysica et Geodetica, v. 34, p. 327–341.

Ising, G., 1942, On the magnetic properties of varved clay: Arkiv For Matematik, Astronomi Och Fysik, v. 29, p. 1–37.

Jeffrey, G., 1922, The motion of Ellipsoidal Particles Immersed in a **V**iscous Fluid: Proceedings of the Royal Society, London, Serial A., v. 102, p. 161–179.

Jelinek, **V**., 1978, Statistical processing of anisotropy of magnetic susceptibility measured on groups of specimens: Studia Geophysica et Geodetica, v. 22, p. 50–62.

Kanamatsu, T., Herrero-Ervera, E., and Taira, A. 2001, Magnetic fabrics of soft-sediment folded strata within a Neogene accretionary complex, the Miura group, central Japan: Earth Planetary Science Letters, v. 187, p. 33–343.

Kennedy, M.P., 1975, Geology of the San Diego Metropolitan Area, California: California Division of Mines and Geology Bulletin, v. 200, 39 p.

Kono, M., 1980, Statistics of paleomagnetic inclination data: Journal of Geophysical Research, v. 85, p. 3879–3882.

Lohmar, J.M., May, J.A., Boyer, J.E., and Warme, J., 1979, Shelf edge deposits of the San Diego embayment: in Eocene Depositional Systems, edited by P.L. Abbott, Los Angeles, USA, The Pacific Section of the Society of Economic Paleontologists and Mineralogists, p. 15–27.

May, J.A., and Warme, J., 1991, Marine sedimentology of the early to middle Eocene La Jolla group: in Eocene Geologic History San Diego Region, edited by P.L. Abbott and J.A. May, Los Angeles, USA, The Pacific Section of the Society of Economic Paleontologists and Mineralogists, v. 68, p. 73–88.

McFadden, P.L., Reid, A.B., 1982, Analysis of paleomagnetic inclination data: Geophysical Journal of the Royal Astronomical Society, v. 69, p. 307–319.

Owens, W.H., 1974, Mathematical model studies on factors affecting the magnetic anisotropy of deformed rocks: Tectonophysics, v. 24, p. 115–131.

Pares, J., van der Pluijm, B., and Dinares-turell, J., 1999, Evolution of magnetic fabrics during incipient deformation of mudrocks (Pyrenes, northern Spain): Tectonophysics, v. 307, p. 1–14.

Rees, A.I., 1965, The use of anisotropy of magnetic susceptibility in the estimation of sedimentary fabric: Sedimentology, v. 4, p. 257–271.

Rosenbaum, J., Reynolds, R., Smoot, J., and Meyer, R., 2000, Anisotropy of magnetic susceptibility as a tool for recognizing core deformation: Reevaluation of the paleomagnetic record of Pleistocene sediments from drill hole OL-92, Owens Lake, California: Earth Planetary Science Letters, v. 178, p. 415–424.

Shor, A.N., Kent, D.V., and Flood, R.D., 1984, Contourite or turbidite?: Magnetic fabric of fine-grained Quaternary sediments, Nova Scotia continental rise Fine-grained sediments: Deep Water Processes and Facies, in Fine-grained sediments: Deep water processes and facies: edited by D. Stowe and D. Piper, p. 257–273, Blackwell Scientific Publications.

Tauxe, L., 1998, Paleomagnetic Principles and Practice: Kluwer Academic Publishers. Boston, USA, 299 p.

FIGURE CAPTIONS

Figure 1. Photographs of slumped outcrop of Ardath Shale north of Scripps Pier at 32°52’05.6”N, 117°15’13.2”W. A: Prominent slump; view to the north. B: Context of site A above slump; view to the east. C: Context of sites B and C, within and below slump, respectively; view to the east.

Figure 2. AMS and paleomagnetic data for the three sites being studied. A–C: AMS eigenvector orientations. Squares are eigenvectors $\mathbf{V}_1$ associated with maximum eigenvalues (τ_1). Triangles are eigenvectors $\mathbf{V}_2$ associated with intermediate eigenvalues (τ_2), and circles are eigenvectors $\mathbf{V}_3$ associated with minimum eigenvalues (τ_3). These are lower-hemisphere, equal-area projections for (A) site A (undeformed), (B) site B (crypto-slump), and (C) site C (slumped) specimens. D–F: Bootstrapped AMS eigenvector

distributions (see text). G–I: Histograms of bootstrapped eigenvalues and 95% confidence bounds. Note that scales for histograms are different for each plot. J–L: Lower-hemisphere, equal-area projections of NRM directions and representative vector-endpoint diagrams for three sites.

Site	$\overline{D}$	$\overline{I}$	N	R	κ	α_{95}
Site A	0.0	54.9	22	21.54	45.3	4.7
Site B	6.0	46.4	12	11.81	57.5	5.8
Site C	1.9	70.3	18	17.22	21.8	7.6

Table 1. Summary of Fisher (1953) statistics for NRM directions shown in Figure 2.


a)
Site A
Sites B & C

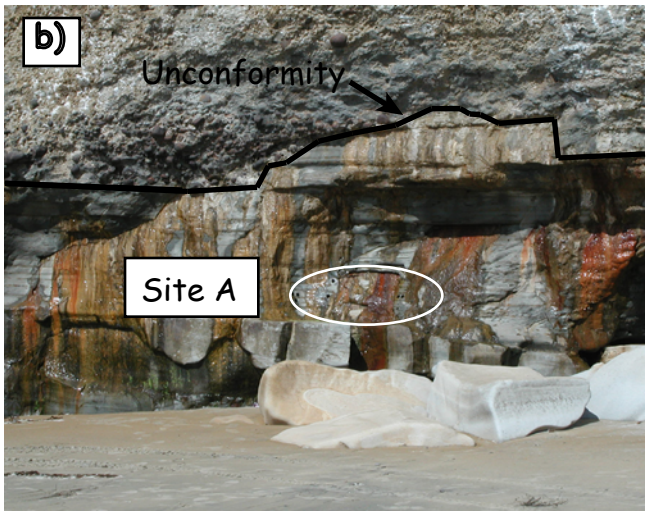
b)
Unconformity
Site A

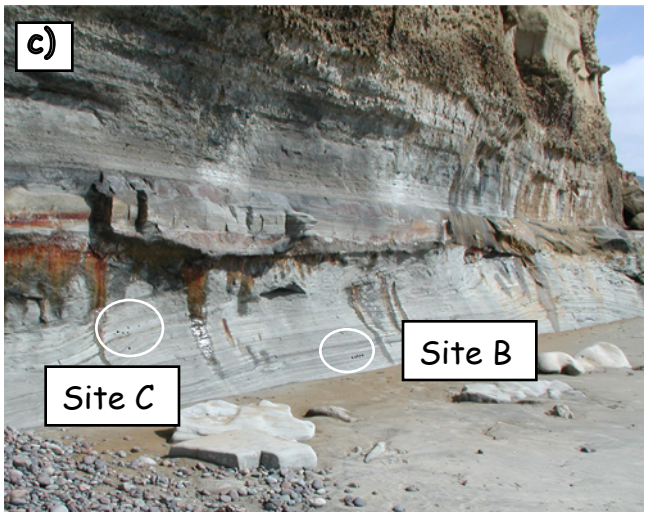
c)
Site B
Site C

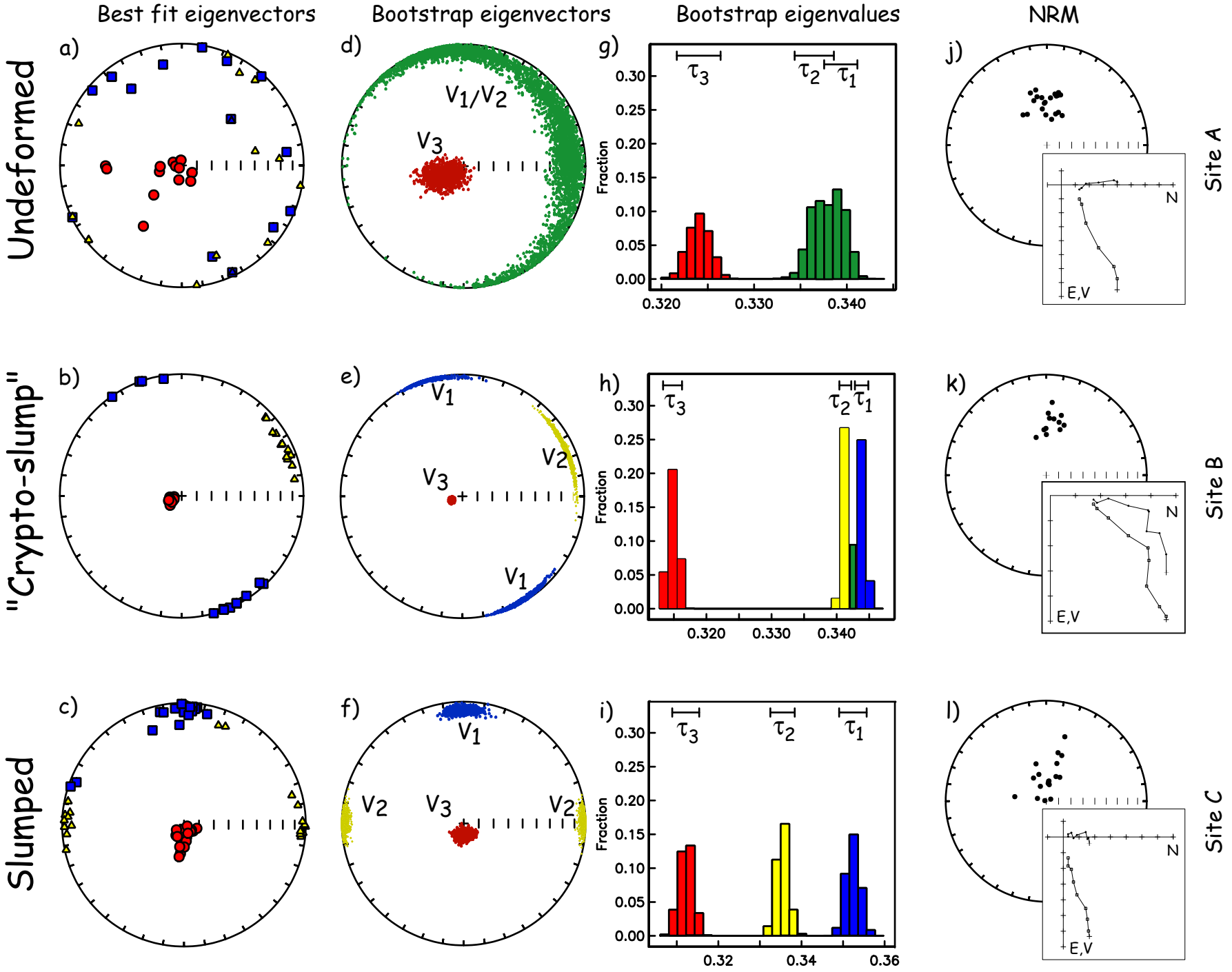
Best fit eigenvectors
Bootstrap eigenvectors
Bootstrap eigenvalues
NRM
Undeformed
"Crypto-slump"
Slumped
Site A
Site B
Site C
a)
b)
c)
d)
e)
f)
g)
h)
i)
j)
k)
l)
V1/V2
V3
V1
V2
τ3
τ2
τ1
Fraction
0.320
0.330
0.340
0.32
0.34
0.36
N
E,V